Title
Fragmentation of wind-blown snow crystals

Journal
Geophysical Research Letters, 44(9)

ISSN
0094-8276

Authors
Comola, Francesco
Kok, Jasper F
Gaume, Johan
et al.

Publication Date
2017-05-16

DOI
10.1002/2017gl073039

Peer reviewed

Fragmentation of wind-blown snow crystals

Francesco Comola[1], Jasper F. Kok[2], Johan Gaume[1,3], Enrico Paterna[3], and Michael Lehning[1,3]

[1]Swiss Federal Institute of Technology, School of Architecture, Civil and Environmental Engineering, Lausanne, Switzerland.

[2]University of California, Department of Atmospheric and Oceanic Sciences, Los Angeles, California.

[3]WSL Institute for Snow and Avalanche Research SLF, Davos, Switzerland

Understanding the dynamics driving the transformation of snowfall crystals into blowing-snow particles is critical to correctly account for the energy and mass balances in polar and alpine regions. Here, we propose a fragmentation theory of fractal snow crystals that explicitly links the size distribution of blowing snow particles to that of falling snow crystals. We use discrete element modeling of the fragmentation process to support the assumptions made in our theory. By combining this fragmentation model with a statistical-mechanics model of blowing-snow, we are able to reproduce the characteristic features of blowing-snow size distributions measured in the field and in a wind tunnel. In particular, both model and measurements show the emergence of a self-similar scaling for large particle sizes and a systematic deviation from this scaling for small particle sizes.

1. Introduction

The size of snow surface particles plays an outsize role in determining the radiative balance [Flanner and Zender, 2006] in polar and alpine regions. A key factor that determines the size distribution of snow particles is the transformation of snowflakes once they impact the surface. In particular, measurements [Sato et al., 2008] show that, even in light winds, many snowflakes break upon collision with the surface, and that the number of fragments increases with impact velocity. Fragmentation of snow crystals blown by wind might explain the remarkable differences in size between snowflakes and blowing snow particles [Gunn and Marshall, 1958; Schmidt, 1982]. Snowfall crystals are relatively large, often in the range of $1 \sim 5$ mm depending on precipitation intensity, and generally follow an exponential size distribution [Woods et al., 2008; Garrett and Yuter, 2014]. In contrast, blowing-snow particles span the size range $50 \sim 500$ μm with a frequency distribution well described by a gamma function [Nishimura and Nemoto, 2005; Nishimura et al., 2014].

Measurements [Legagneux et al., 2002] suggest that, when wind shatters large dendritic crystals into small fragments, the specific surface area of a fresh snow cover significantly decreases. Because specific surface area has been identified as one of the main controls on the optical properties of snow surfaces [Domine et al., 2006], blowing-snow fragmentation may significantly reduce snow surface albedo in alpine and polar regions, and thus play a key role in the energy budget. Furthermore, the size-distribution of deposited snow partially determines the mechanical properties of alpine snow covers and thus their vulnerability to wind erosion [Gallée et al., 2001] and avalanche danger [Gaume et al., 2017]. Moreover, fragmentation processes intensify snow sublimation, which is not only responsible for a significant loss of snow mass in snow-covered regions [Lenaerts et al., 2012; MacDonald et al., 2010], but also for bromine aerosols release and seasonal ozone depletion in Antarctica [Yang et al., 2008; Lieb-Lappen and Obbard, 2015].

Here, we propose that fragmentation of snow particles while they are blown by wind is the missing link that connects the size distribution of precipitating snowflakes to that of deposited snow crystals. Specifically, we propose a physical and mathematical description of snow fragmentation, based on the fractal geometry of dendritic snow crystals. We evaluate the assumptions of the theory through discrete element simulations of snow crystal breaking. We finally derive and apply a statistical-mechanics model of saltation, which incorporates the proposed fragmentation processes, to establish the missing connection between snowfall and blowing-snow size-distributions.

2. Snow crystal fragmentation

When wind blows over a fresh snow cover, snow crystals are lifted through aerodynamic or splash entrainment [Clifton and Lehning, 2008; Comola and Lehning, 2017], follow ballistic trajectories in the saltation layer and eventually impact the surface, thereby producing smaller fragments [Sato et al., 2008]. Large fragments follow the same dynamics, break further and progressively gain momentum until they are small enough to be transported in suspension by turbulent eddies [Pomeroy and Gray, 1990]. These fragmentation processes are controlled by the kinetic energy and mechanical properties of the wind-blown sediment [Kok, 2011]. When subjected to impulsive forces, ice behaves as a brittle material [Kirchner et al., 2001; Weiss, 2001], presenting a linearly elastic response up to a failure stress at which fracture occurs. In brittle objects, such as ice solids, crack propagation dynamics depend on the impact energy. Low energies generate the so-called damage regime, yielding a few fragments having size of the same order of the original object, while high energies produce the so-called shattering regime, yielding a full scale-invariant spectrum of fragment sizes [Kun and Herrmann, 1999].

The fragmentation dynamics of snow crystals are likely to be different from those of ice solids, in large part because of the uncertain role played by their geometry. It is known that snow crystals present extremely variable shapes, such as needles, columns, plates, and dendrites, depending on temperature and humidity at the time of formation [Nakaya, 1954]. Because of such fascinating diversity, the development of a fragmentation theory that applies to any crystal type seems prohibitive. Nevertheless, there exists a family of snow crystals that present a common feature, that is, a fractal structure. A typical example are the dendritic crystals, which mostly form in conditions of supersaturation and temperature ranges $-22 \sim -10$ °C and $-3 \sim 0$ °C [Nakaya, 1954]. Dendritic crystals are commonly observed in nature. It should not surprise, in fact, that one of earliest fractal shapes to have been described is the so-called "Koch's snowflake" [Sugihara and May, 1990]. Numerical and experimental studies were able to identify the fractal dimension γ of dendritic snow crystals, which spans the range $1.9 \sim 2.5$ depending on their specific structure [Nittmann and Stanley, 1987; Heymsfield et al., 2010; Chukin et al., 2012; Leinonen and Moisseev, 2015]. We hereafter exploit the fractal properties of dendritic snow crystals to derive a fragmentation theory that links the size distribution of snowfall crystals to that of blowing-snow particles.

When a fractal crystal impacts the surface with sufficient energy, crack formation is likely to take place at the connections between different branches, where sharp corners yield local stress peaks. Accordingly, a fundamental role is played by the size distribution of surface irregularities. Let us define the box-counting measure $M(\epsilon)$ as the number of boxes of side-length ϵ needed to cover the fractal curve. A relevant property of fractals is the scale invariance of the box-counting measure, i.e. $M(\lambda\epsilon) = \lambda^{-\gamma} M(\epsilon)$ [Weiss, 2001]. Let us then call D the size of the parent crystals, which is commonly defined as the diameter of the circle of equivalent area [Schmidt, 1982; Nishimura and Nemoto, 2005; Gordon and Taylor, 2009], and λD the distance between adjacent cracks, with $\lambda \in [0;1]$. Assuming that cracks develop from sharp corners, where small curvatures yield local stress peaks, crystal breaking acts by chipping surface irregularities off the fractal contour. Because the distance between adjacent cracks defines the characteristic size of the fragment, λ is hereafter referred to as the dimensionless fragment size. The fragment size distribution resulting from the complete shattering of the fractal crystal would be perfectly scale-invariant, such that the number $N(\lambda D)$ of fragments with size λD is $\lambda^{-\gamma} N(D)$. Given that we are considering only one parent crystal, we would have $N(D) = 1$ and $N(\lambda D) = \lambda^{-\gamma}$. However, it is sensible to assume that impact energies are generally not large enough to yield a complete shattering, but rather a damage regime characterized by crack formation at a few critical corners. Let us then call $p(\lambda)$ the probability density function describing the likelihood of crack formations at distance λD one from another. The total number of children crystals formed upon impact is therefore

$$N = \int_0^1 N(\lambda D)\,\mathrm{d}\lambda = \int_0^1 \lambda^{-\gamma} p(\lambda)\,\mathrm{d}\lambda. \quad (1)$$

Equation (1) can be employed to estimate the number of fragments produced upon impact of a dendritic snow crystal, provided some reasonable assumptions on the probability distribution $p(\lambda)$ are made. Even though $p(\lambda)$ is not precisely known, it seems reasonable to assume that cracks develop from the sides of larger branches, which are more protruding and thus more subjected to large bending forces and local stress peaks. If we indicate with Λ the size of the larger branches, this assumption yields $p(\lambda) = \delta(\lambda - \Lambda)$, i.e., a Dirac delta function centered in Λ, such that

$$N = \Lambda^{-\gamma}. \quad (2)$$

We perform numerical simulations of snow crystal fragmentation based on the discrete element method (DEM) to evaluate whether equation (2) holds for a dendritic snow crystal. Figure 1a (ii) shows the simplified snow crystal model, whose geometry mimics that of a real dendritic snowflake (Figure 1a (i)), formed of ice elements in contact through cohesive bonds (see also Figure S1 of the supporting information). The mechanical properties of ice are used for the contact model [Petrovic, 2003; Gaume et al., 2015], yielding realistic deformations and stress distribution (details about the DEM are provided in section 1 of the supporting information [Cundall and Strack, 1979; Akyildiz et al., 1990; Itasca Consulting Group, 2014; Steinkogler et al., 2015]).

We perform impact simulations with a flat surface for different values of impact speed v_i and impact angle θ_i, computing the stress distribution (Figure 1a (iii)) and the fragment release (Figure 1a (iv)). Although the DEM approach would allow us to investigate the fragmentation process in three dimensions, such simulations would present additional degrees of freedom and require information on the three-dimensional structure of the snowflake. Because our purpose is to test a fragmentation theory derived from the fractal properties of planar snowflakes, we chose to perform 2-D simulations to provide the best trade-off between accuracy and complexity.

Figure 1b shows the cumulative distribution (CD) and the frequency distribution (FD, in the inset) of the fragment sizes. We obtain the distributions from averaging the results of 1000 impact simulations, presenting all possible combinations of 10 values of crystal orientation $\beta_i \in [0°, 60°]$ (see Figure 1a (ii)), 10 values of impact velocity $v_i \in [0.5, 1.5]$ m/s, and 10 values of impact angle $\theta_i \in [5°, 15°]$. The variability ranges of v_i and θ_i are typical of snow saltation [Araoka and Maeno, 1981]. The frequency distribution highlights that the majority of fragments presents $\lambda = 0.2 \sim 0.3$, with a mean value $\langle\lambda\rangle = 0.3$. If we assign $\Lambda = 0.3$ in equation (2) it follows that, for a fractal dimension $\gamma = 2.1$ repersentative of dendritic shapes, the number of fragments N is approximately 10.

Figures 1c and 1d show how $\langle\lambda\rangle$ and N vary with respect to impact velocity v_i and impact angle θ_i. Each value of $\langle\lambda\rangle$ and N is obtained by averaging the results of 10 impact simulations with different crystal orientations β_i. These results suggest that $\langle\lambda\rangle \approx 0.3$ and $N \approx 10$ are reasonable approximations in the range of impact velocities and impact angles typical of snow saltation [Araoka and Maeno, 1981] (we study the sensitivity of our results to these values in section 5).

The DEM simulations thus suggest that equation (2) provides an effective prediction on the number of fragments produced upon breaking of a dendritic crystal. The results also indicate that crystal rebound does not take place under the tested impact conditions and that deposition only occurs for very low impact velocities ($\langle\lambda\rangle = 1$ and $N = 0$ for $v_i < 0.2$ ms^{-1}, Figure 1c), which is consistent with experimental observations [Sato et al., 2008].

3. Blowing-snow fragmentation

In light of the observations of section 2, we propose a physical description of blowing-snow fragmentation as schematically represented in Figure 2. A large dendritic snowflake of size D_0, lifted from the surface through aerodynamic or splash entrainment, follows a ballistic trajectory and eventually impacts the surface producing a number $N = \Lambda^{-\gamma}$ of smaller fragments with size $D_1 = \Lambda D_0$. A fraction $\alpha\left(D_1\right)$ of these children crystals moves to the suspension layer transported by turbulent eddies, while the remaining part remains in saltation and eventually impacts the surface generating fragments of size $D_2 = \Lambda D_1$. Given that crystals of size D_2 have a smaller inertia than crystals of size D_1, turbulent motions are more efficient in carrying them in suspension and thus $\alpha\left(D_2\right) > \alpha\left(D_1\right)$. Following this fragmentation pattern, the number of crystals of size $D_n = \Lambda D_{n-1}$ generated at the n^{th} impact is

$$N\left(D_n\right) = N\left(D_{n-1}\right)\left[1 - \alpha\left(D_{n-1}\right)\right]\Lambda^{-\gamma}. \tag{3}$$

An assumption underlying the proposed theory is the scale-invariance of the fragmentation process, that is, children crystals of any size present the same fractal geometry and thus experience the same fragmentation dynamics of their larger parent crystals. The experimental studies by Sato et al. [2008] and our DEM simulations (Figure 1) suggest that large crystals are too brittle to rebound without breaking and that deposition occurs in very light wind conditions, i.e., for surface shear stresses significantly below the limit required to initiate snow transport. Accordingly, we assume that crystals of any size experience fragmentation upon impact, neglecting deposition and rebound. In reality, crystal fragments with size of the order of the smallest branches (around 50 μm) present a spheroidal shape rather than a fractal one [Gordon and Taylor, 2009]. Small-scale deviations from the fractal theory are, in fact, typical of all geometries of nature [Brown et al., 2002]. The saltation dynamics of small ice fragments become then similar to those of sand grains, which experience deposition and rebound rather than fragmentation [Kok et al., 2012; Kobayashi, 1972]. Bearing this limitation in mind, we can still regard the assumption of scale-invariance as adequate for the purpose of studying how fragmentation processes transform the snowfall size-distribution, given the significant separation between the size of large snowflakes and the length scale at which the fractal theory is expected to fail.

4. Modeling blowing-snow fragmentation

We incorporate the proposed fragmentation process in a statistical-mechanics model of saltation. We cast the particle dynamics in a residence time distribution framework, which has been widely employed in stochastic formulations of water [Botter et al., 2011], contaminant [Benettin et al., 2013], and heat transport [Comola et al., 2015] in underground formations. Let us define the residence time of a crystal as the time elapsed between the start and the end of its motion in the saltation layer. Crystal motion can start when the crystal is entrained from the surface, through aerodynamic forces or splash, or when the crystal is formed upon fragmentation of a larger crystal. Conversely, the end of motion occurs when the crystal moves to the suspension layer carried by turbulence or when it impacts the surface, producing smaller fragments.

The number $N(D,t)$ (m^{-2}) of crystals of size D in saltation at time t can be expressed as the number of crystals whose motion starts at time t' and whose residence time is larger than $t-t'$, for all $t'<t$, i.e.

$$N(D,t) = \int_0^t \left[E(D,t) + F(D,t)\right] P(t-t' \mid D)\, \mathrm{d}t'. \tag{4}$$

$E(D,t)$ and $F(D,t)$ ($\mathrm{m}^{-2}\mathrm{s}^{-1}$) are surface entrainment and fragment production, i.e. the fluxes responsible for initiating crystal motion. $P(t-t' \mid D)$ is the probability that the residence time of crystals of size D is larger than $t-t'$. We can differentiate equation (4) using Leibniz's rule to express the size-resolved mass balance equation (see section 2 of the supporting information for more details)

$$\frac{\mathrm{d}N(D,t)}{\mathrm{d}t} = E(D,t) + F(D,t) - S(D,t) - I(D,t). \tag{5}$$

On the right-hand side of equation (5), the two sink terms $S(D,t)$ and $I(D,t)$ ($\mathrm{m}^{-2}\mathrm{s}^{-1}$) are the suspension flux and the impact rate of crystals of size D at time t. These two terms read

$$S(D,t) = \alpha(D) \int_0^t \left[E(D,t') + F(D,t')\right] p_S(t-t')\, \mathrm{d}t', \tag{6}$$

$$I(D,t) = [1-\alpha(D)] \int_0^t [E(D,t') + F(D,t')]\, p_I(t-t')\, \mathrm{d}t'. \tag{7}$$

$\alpha(D) \in [0;1]$ is the probability that a crystal of size D becomes suspended. Conversely, $1-\alpha(D)$ is the probability that a crystal of size D impacts the surface. Here, we assign to $\alpha(D)$ the expression of the eddy-diffusivity correction for inertial particles with respect to passive tracers [Csanady, 1963], given that the two quantities obey the same limits and are governed by similar physics. In fact, the probability of becoming suspended is equal to 1 in the limit of $D \to 0$, that is, for passive tracers, decreases as the settling velocity becomes relevant compared to turbulent fluctuations, and reaches the lower value 0 in the limit of $D \to \infty$. We therefore write

$$\alpha(D) = \left[1 + \frac{w_s^2(D)}{\sigma^2}\right]^{-\frac{1}{2}}, \tag{8}$$

where $w_s(D)$ is the settling velocity of crystals of size D and σ^2 is the turbulence velocity variance (see section 2 of the supporting information for their analytical expressions [Pope, 2001; Stull, 2012]). Furthermore, $p_S(t-t')$ and $p_I(t-t')$ are the residence-time probability density functions of crystals moving to suspension and impacting the surface, respectively. If we assume that particles move independently from one another, it follows that the dynamics are well described by a Poisson process, yielding for $p_S(t-t')$ and $p_I(t-t')$ exponential residence time distributions.

We assume that the surface entrainment $E(D,t)$, the first source term on the right-hand side of equation (5), samples uniformly from the size-distribution of crystals resting at the surface, according to the principle of equal mobility [Willetts, 1998]. Because we aim at establishing a link between the snowfall and blowing-snow size distributions, we consider the typical situation in which drifting snow already starts during snowfall events. We therefore simulate impact and fragmentation of snowfall crystals by applying equation (1) to an exponential snowfall size-distribution bounded within 0.75 and 2 mm (dashed black line in Figure S4 of the supporting information), which is typical of precipitation intensities of the order of ~ 0.3 mmh^{-1} [Gunn and Marshall, 1958]. The resulting size-distribution of surface crystals proves similar to that obtained by sieve analysis in very cold conditions [Granberg, 1985] (dashed grey line in Figure S4 of the supporting information). It does happen, sometimes, that low-wind snowfalls generate a snow cover that is eroded by subsequent higher winds. In these cases, the size distribution of surface particles does not only result from fragmentation of snowfall crystals, but also from the snow metamorphism that takes place in the snow cover [Colbeck, 1982]. Although relevant in some situations, the effect of snow metamorphism goes beyond the scope of this work and is thus not included in our model.

The second source term in equation (5) is the fragment production rate $F(D,t)$, which, following equation (1), reads

$$F(D,t) = \int_0^1 I\left(\frac{D}{\lambda},t\right)\lambda^{-\gamma}p(\lambda)\,\mathrm{d}\lambda. \tag{9}$$

If we assume again that $p(\lambda) = \delta(\lambda - \Lambda)$, we obtain $F(D,t) = I(D/\Lambda,t)\,\Lambda^{-\gamma}$.

We solve equation (5) numerically, letting the system evolve until a stationary condition is reached (see section 3 of the supporting information for more details on the transient process). We then compute the size-distribution of blowing-snow by normalizing $N(D,t)$ in stationary conditions.

5. Model results

We first perform a model simulation using $\gamma = 2.1$ and $\Lambda = 0.3$, which are representative of the dendritic snow crystal considered in section 2. In our simulations, we set a lower threshold of 10 µm to the particle size, assuming that any smaller crystal disappears through sublimation. To evaluate the model results, we analyze all known published datasets of blowing-snow size distributions, collected from field campaigns in the United States [Schmidt, 1982], Canada [Gordon and Taylor, 2009], French Alps [Nishimura et al., 2014], and Antarctica [Nishimura and Nemoto, 2005] (see section 5 of the supporting information for more details). It is worth noting that the snowflake shape for the different measurements is unknown, and likely presents a mix of fractal and non-fractal snow types.

We only consider size-distribution measurements within the saltation height, which is approximately of the order of 15 cm [Gordon et al., 2009; Nishimura and Nemoto, 2005]. If several saltation measurements are available for the same dataset, we average them to obtain the mean size-distribution. Additionally, we present the blowing-snow size-distribution that we measured in wind tunnel tests. We carried out the experiments over a post-snowfall surface at the Institute for Snow and Avalanche Research (SLF/WSL) in Davos, Switzerland, at 1670 m above sea level [Clifton et al., 2006]. We obtain the blowing-snow size-distribution by averaging three series of measurements within the saltation layer, namely at 10, 17, and 30 mm above the surface.

Figure 3 shows the size-distribution $\mathrm{d}N/\mathrm{d}D$ as obtained from the fragmentation model (grey dashed line) and dataset analyses (colored dots). The measured size-distributions, which are commonly approximated by a gamma function, are well reproduced by the proposed fragmentation theory. In particular, results highlight that blowing-snow size-distributions display a power-law scaling for the largest crystal sizes ($D > 200$ μm) and a systematic deviation from this self-similar scaling for smaller sizes. Interestingly, the power-law exponent seems to be approximately 2.1, suggesting that the fractal dimension is indeed a control on snow crystal fragmentation. The deviation from the power-law indicates that there exists an under-production of fragments smaller than 200 μm, that is, not all the small branches are chipped off the crystal contour. In fact, as shown in Figure 2, the fragmentation process yields small fragments only after multiple impacts, when a significant number of the larger fragments has already moved to suspension with smaller branches still attached. It is worth noting, however, that the small-scale deviation observed in the measured size-distributions may in part be due to the rapid sublimation of the smallest ice fragments [Groot Zwaaftink et al., 2011].

The results thus suggest that a fractal power-law scaling emerges in the size range for which turbulent eddies are not efficiently carrying crystals in suspension ($200 - 500$ μm). On the contrary, below 200 μm, turbulence starts to be efficient in removing crystals from the saltation layer and reducing the production of smaller fragments. As a result, the peak of the blowing-snow size-distributions lies at ~ 100 μm, where there is the optimal trade-off between the two described mechanisms.

We further perform a sensitivity analysis of the model results to variations in the fractal dimension γ, within the range suggested by measurements, and fragment size Λ, within the range suggested by the DEM simulations. The purpose of this analysis is to test whether variations in the dendritic structure (different γ values) and in the impact conditions (different Λ values) may significantly alter the blowing-snow size distribution. Figures 3b and 3c suggest that varying γ and Λ produces significant quantitative variations in the results. Despite this quantitative sensitivity, the main qualitative features of the results seem robust relative to reasonable variations in γ and Λ.

6. Discussion and conclusions

We proposed a fragmentation theory for snow crystals to test the hypothesis that fragmentation processes constitute the missing link between the seemingly inconsistent size distributions of snowfall and blowing-snow. A key assumption underlying our model is that the fragment size and the fragment number follow from the power-law distribution of surface irregularities typical of fractal geometries. We used discrete element simulations of snow crystal breaking to explicitly test this assumption. These simulations indicated that the theoretical results in terms of fragment size and number is indeed representative of a dendritic snowflake geometry (Figure 1). The results of a statistical-mechanics model of saltation, accounting for the proposed fragmentation theory, are consistent with measurements (Figure 3a).

Our results suggest that the self-similarity of snow crystals shapes the blowing-snow size-distribution. In particular, our model predicts, and measurements support, a self-similar scaling for crystal sizes larger than 200 μm (Figure 3). The deviation from the power-law observed at the lower end of crystal size is due to the relatively large turbulent-diffusivity of particles smaller than 200 μm, which are efficiently transported in suspension and are thus less likely to produce smaller fragments upon impact.

Overall, our analysis suggests that fragmentation processes can indeed transform an exponential snowfall distribution into the so-called gamma distribution of blowing-snow. In particular, the typical features of a gamma distribution emerge, on one side, from the fractal geometry and, on the other side, from the interactions between inertial particles and turbulent eddies.

Further analyses show that these features are conserved for a wide range of fractal dimensions and fragment sizes (Figures 3b and 3c). This suggests that the proposed fragmentation dynamics may hold for a wide range of dendritic snowflakes and impact conditions. It is worth noting that some commonly observed snow crystals, such as needles and plates, do not present the fractal structure considered in our theory. Figure 3a indicates, however, that our model can reproduce several measured size distributions, which may have resulted from fragmentation of snowflakes with different shapes. This suggests that our theory may still provide an effective prediction of the size and number of fragments produced by non-dendritic crystals, although the assumptions on which the theory rests are not supposed to hold for these shapes.

Our work also points toward the need of accurate estimations for the typical time- and length-scale necessary to complete the transition from the size-distribution of snowfall to that of blowing-snow. This will clarify the need of accounting for fragmentation processes in snow transport models and in climate models, in order to improve the predictions of surface mass and energy balances in snow-covered regions.

7. Acknowledgments

We acknowledge the Swiss National Science Foundation for supporting the measurement equipment (R'Equip grant No.206021_133786) and the wind tunnel facility (R'Equip grant No. 2160_060998). Johan Gaume has been supported by the Ambizione grant of the Swiss National Science Foundation (PZ00P2 161329). All data used in this study will be made available upon request.

References

F. Akyildiz, R. Jones, and K. Walters. On the spring-dashpot representation of linear viscoelastic behaviour. *Rheol. Acta*, 29(5):482–484, 1990.

K. Araoka and N. Maeno. Dynamical behaviors of snow particles in the saltation layer. *Mem. Natl. Inst. Polar Res., Special Issue.*, 19:253–263, 1981.

P. Benettin, Y. Velde, S. E. Zee, A. Rinaldo, and G. Botter. Chloride circulation in a lowland catchment and the formulation of transport by travel time distributions. *Water Resour. Res.*, 49(8):4619–4632, 2013.

G. Botter, E. Bertuzzo, and A. Rinaldo. Catchment residence and travel time distributions: The master equation. *Geophys. Res. Lett.*, 38(11), 2011.

J. H. Brown, V. K. Gupta, B.-L. Li, B. T. Milne, C. Restrepo, and G. B. West. The fractal nature of nature: power laws, ecological complexity and biodiversity. *Phil. Trans. R. Soc. B*, 357(1421):619–626, 2002.

V. Chukin, D. Mikhailova, and V. Nikulin. Two methods of determination of ice crystal fractal dimension. *Science Prospects*, 9(36):5–7, 2012.

A. Clifton and M. Lehning. Improvement and validation of a snow saltation model using wind tunnel measurements. *Earth Surf. Process. Landf.*, 33(14):2156–2173, 2008.

A. Clifton, J.-D. Rüedi, and M. Lehning. Snow saltation threshold measurements in a drifting-snow wind tunnel. *J. Glaciol.*, 52(179):585–596, 2006.

S. Colbeck. An overview of seasonal snow metamorphism. *Rev. Geophys.*, 20(1):45–61, 1982.

F. Comola and M. Lehning. Energy- and momentum-conserving model of splash entrainment in sand and snow saltation. *Geophys. Res. Lett.*, 44:1–9, 2017.

F. Comola, B. Schaefli, A. Rinaldo, and M. Lehning. Thermodynamics in the hydrologic response: Travel time formulation and application to Alpine catchments. *Water Resour. Res.*, 51(3):1671–1687, 2015.

G. Csanady. Turbulent diffusion of heavy particles in the atmosphere. *J. Atmos. Sci.*, 20 (3):201–208, 1963.

P. A. Cundall and O. D. L. Strack. A discrete numerical model for granular assemblies. *Géotechnique*, 29:47–65, 1979.

F. Domine, R. Salvatori, L. Legagneux, R. Salzano, M. Fily, and R. Casacchia. Correlation between the specific surface area and the short wave infrared (SWIR) reflectance of snow. *Cold Reg. Sci. Technol.*, 46(1):60–68, 2006.

M. G. Flanner and C. S. Zender. Linking snowpack microphysics and albedo evolution. *J. Geophys. Res.*, 111(D12), 2006.

H. Gallée, G. Guyomarc'h, and E. Brun. Impact of snow drift on the antarctic ice sheet surface mass balance: possible sensitivity to snow-surface properties. *Boundary-Layer Meteorol.*, 99(1):1–19, 2001.

T. J. Garrett and S. E. Yuter. Observed influence of riming, temperature, and turbulence on the fallspeed of solid precipitation. *Geophys. Res. Lett.*, 41(18):6515–6522, 2014.

J. Gaume, A. Van Herwijnen, G. Chambon, K. Birkeland, and J. Schweizer. Modeling of crack propagation in weak snowpack layers using the discrete element method. *Cryosphere*, 9(5):1915–1932, 2015.

J. Gaume, A. van Herwijnen, G. Chambon, N. Wever, and J. Schweizer. Snow fracture in relation to slab avalanche release: critical state for the onset of crack propagation. *Cryosphere*, 11(1):217–228, 2017.

M. Gordon and P. A. Taylor. Measurements of blowing snow, part I: Particle shape, size distribution, velocity, and number flux at Churchill, Manitoba, Canada. *Cold Reg. Sci. Technol.*, 55(1):63–74, 2009.

M. Gordon, S. Savelyev, and P. A. Taylor. Measurements of blowing snow, part II: Mass and number density profiles and saltation height at Franklin Bay, NWT, Canada. *Cold Reg. Sci. Technol.*, 55(1):75–85, 2009.

H. Granberg. Distribution of grain sizes and internal surface area and their role in snow chemistry in a sub-Arctic snow cover. *Ann. Glaciol.*, 7:149–152, 1985.

C. Groot Zwaaftink, H. Löwe, R. Mott, M. Bavay, and M. Lehning. Drifting snow sublimation: A high-resolution 3-D model with temperature and moisture feedbacks. *J. Geophys. Res.*, 116(D16), 2011.

K. Gunn and J. Marshall. The distribution with size of aggregate snowflakes. *J. Meteorol.*, 15(5):452–461, 1958.

A. J. Heymsfield, C. Schmitt, A. Bansemer, and C. H. Twohy. Improved representation of ice particle masses based on observations in natural clouds. *J. Atmos. Sci.*, 67(10): 3303–3318, 2010.

Itasca Consulting Group. *PFC - Particle Flow Code, Ver. 5.0*, 2014.

H. Kirchner, G. Michot, H. Narita, and T. Suzuki. Snow as a foam of ice: plasticity, fracture and the brittle-to-ductile transition. *Philos. Mag. A*, 81(9):2161–2181, 2001.

D. Kobayashi. Studies of snow transport in low-level drifting snow. *Contrib. Inst. Low Temp. Sci.*, 24:1–58, 1972.

J. F. Kok. A scaling theory for the size distribution of emitted dust aerosols suggests climate models underestimate the size of the global dust cycle. *Proc. Natl. Acad. Sci. U.S.A.*, 108(3):1016–1021, 2011.

J. F. Kok, E. J. Parteli, T. I. Michaels, and D. B. Karam. The physics of wind-blown sand and dust. *Rep. Prog. Phys.*, 75(10):106901, 2012.

F. Kun and H. J. Herrmann. Transition from damage to fragmentation in collision of solids. *Phys. Rev. E*, 59(3):2623, 1999.

L. Legagneux, A. Cabanes, and F. Dominé. Measurement of the specific surface area of 176 snow samples using methane adsorption at 77 K. *J. Geophys. Res.*, 107(D17), 2002.

J. Leinonen and D. Moisseev. What do triple-frequency radar signatures reveal about aggregate snowflakes? *J. Geophys. Res.*, 120(1):229–239, 2015.

J. Lenaerts, M. Den Broeke, W. Berg, E. v. Meijgaard, and P. Kuipers Munneke. A new, high-resolution surface mass balance map of Antarctica (1979–2010) based on regional atmospheric climate modeling. *Geophys. Res. Lett.*, 39(4), 2012.

R. Lieb-Lappen and R. Obbard. The role of blowing snow in the activation of bromine over first-year Antarctic sea ice. *Atmos. Chem. Phys.*, 15(13):7537–7545, 2015.

M. MacDonald, J. Pomeroy, and A. Pietroniro. On the importance of sublimation to an alpine snow mass balance in the Canadian Rocky Mountains. *Hydrol. Earth Sys. Sci.*, 14(7):1401–1415, 2010.

U. Nakaya. *Snow crystals: natural and artificial.* Harvard University Press, 1954.

K. Nishimura and M. Nemoto. Blowing snow at Mizuho station, Antarctica. *Phil. Trans. R. Soc. A*, 363(1832):1647–1662, 2005.

K. Nishimura, C. Yokoyama, Y. Ito, M. Nemoto, F. Naaim-Bouvet, H. Bellot, and K. Fujita. Snow particle speeds in drifting snow. *J. Geophys. Res.*, 119(16):9901–9913, 2014.

J. Nittmann and H. E. Stanley. Non-deterministic approach to anisotropic growth patterns with continuously tunable morphology: the fractal properties of some real snowflakes. *J. Phys. A Math. Gen.*, 20(17):L1185, 1987.

J. J. Petrovic. Review mechanical properties of ice and snow. *J. Mater. Sci.*, 38(1):1–6, 2003.

J. Pomeroy and D. Gray. Saltation of snow. *Water Resour. Res.*, 26(7):1583–1594, 1990.

S. B. Pope. Turbulent flows, 2001.

T. Sato, K. Kosugi, S. Mochizuki, and M. Nemoto. Wind speed dependences of fracture and accumulation of snowflakes on snow surface. *Cold Reg. Sci. Technol.*, 51(2):229–239, 2008.

R. Schmidt. Vertical profiles of wind speed, snow concentration, and humidity in blowing snow. *Boundary-Layer Meteorol.*, 23(2):223–246, 1982.

W. Steinkogler, J. Gaume, L. H, B. Sovilla, and M. Lehning. Granulation of snow: from tumbler experiments to discrete element simulations. *J. Geophys. Res.*, 120(6):1107–1126, 2015.

R. B. Stull. *An introduction to boundary layer meteorology*, volume 13. Springer Science & Business Media, 2012.

G. Sugihara and R. M. May. Applications of fractals in ecology. *Trends Ecol. Evol.*, 5(3): 79–86, 1990.

J. Weiss. Fracture and fragmentation of ice: a fractal analysis of scale invariance. *Eng. Fract. Mech.*, 68(17):1975–2012, 2001.

B. Willetts. Aeolian and fluvial grain transport. *Phil. Trans. R. Soc. A*, pages 2497–2514, 1998.

C. P. Woods, M. T. Stoelinga, and J. D. Locatelli. Size spectra of snow particles measured in wintertime precipitation in the Pacific Northwest. *J. Atmos. Sci.*, 65(1):189–205, 2008.

X. Yang, J. A. Pyle, and R. A. Cox. Sea salt aerosol production and bromine release: Role of snow on sea ice. *Geophys. Res. Lett.*, 35(16), 2008.

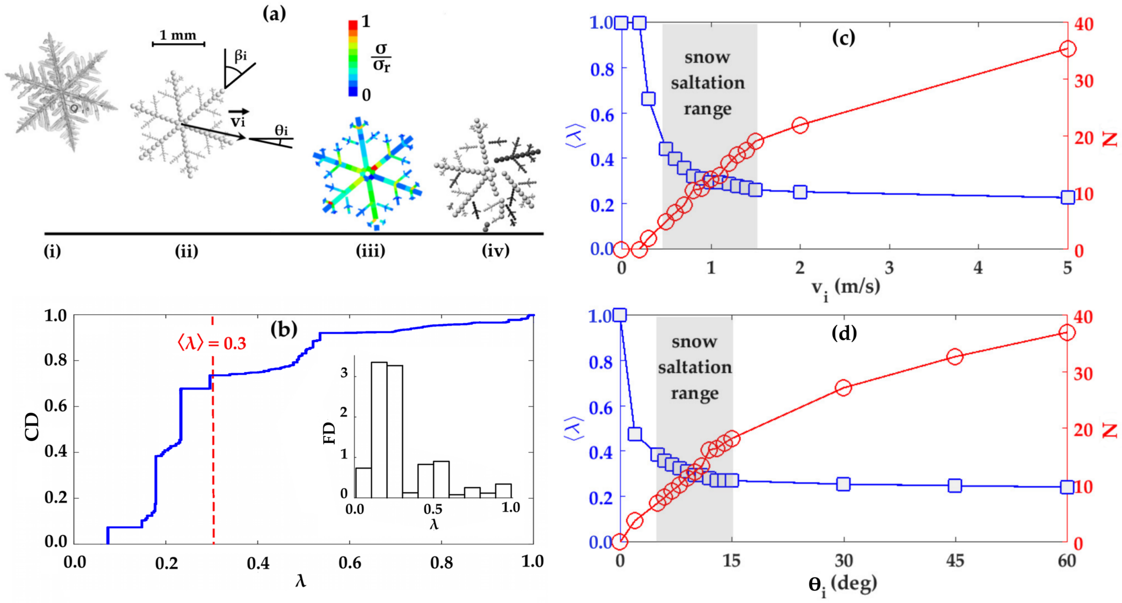

Figure 1. (a) Illustration of the DEM simulations: i) real snowflake (credit: Satoshi Yanagi, http://www1.odn.ne.jp/snow-crystals/page1_E.html), ii) simplified DEM description, iii) ratio between tensile stress σ in bonds and at the moment of the impact and tensile strength of ice σ_r, iv) fragmented snowflake (each level of grey represents a fragment). In the snow crystal model, the radius of the largest elements is 50 µm, while the radius of the smallest ones is 12.5 µm. (b) Cumulative size distribution (CD) of the dimensionless fragment size λ and corresponding frequency distribution (FD). (c) Influence of impact velocity and (d) impact angle on the average dimensionless fragment size $\langle\lambda\rangle$ and number of fragments N. The grey bands identify the ranges of impact velocity and impact angle typical of snow saltation, i.e., $0.5 < v_i < 1.5$ m/s and $5° < \theta_i < 15°$ [Araoka and Maeno, 1981].

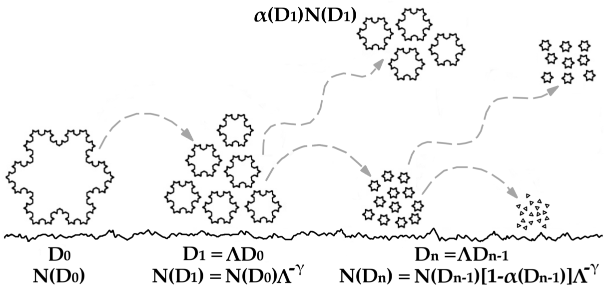

Figure 2. Schematic representation of the fragmentation process during saltation. Each crystal impact leads to formation of fragments having size equal to Λ times the original size. The number of children crystals follows from the scale-invariance property. Small fragments, formed after repeated impacts, are likely to be caught by turbulent eddies and transported to the suspension layer.

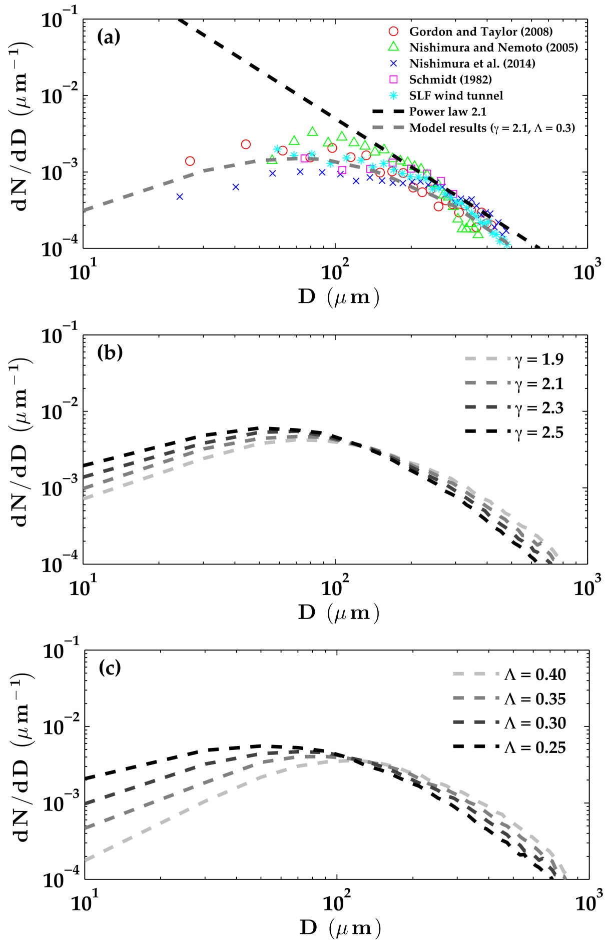

Figure 3. (a) Size-distribution of saltating snow crystals, modeled with the proposed fragmentation theory (dashed grey line), reported in published datasets [Gordon and Taylor, 2009; Nishimura et al., 2014; Nishimura and Nemoto, 2005; Schmidt, 1982], and measured in the SLF wind tunnel in Davos, Switzerland (colored dots). Because the normalized distributions are sensitive to the specific range of sizes measured by the instruments, we rescaled the distributions such that all of them are tangent to a unique power-law (black dashed line) in the range where they show a scale-invariant behavior (200 $\sim$ 500 μm). (b) Sensitivity analysis of the modeled blowing-snow size distribution to the fractal dimension γ. (c) Sensitivity analysis of the modeled blowing-snow size distribution to the dimensionless fragment size Λ.